Nanographene-Based Metal-Organic Framework Thin Films: Optimized Packing and Efficient Electron-Hole Separation Yielding Efficient Photodetector

Zhiyun Xu, Yidong Liu, Abhinav Chandresh, Palas Baran Pati, Vincent Monnier, Lars Heinke, Fabrice Odobel, Stéphane Diring,* Ritesh Haldar,* and Christof Wöll*

Organic semiconductors, specifically polycyclic aromatic chromophores like pentacene, coronene, and nanographenes (hexa-*peri*-hexabenzocoronene, HBC), are often utilized in optoelectronic applications due to their intriguing single-molecule properties. However, the integration of these aromatic compounds into optoelectronic devices frequently encounters significant obstacles, primarily due to the unpredictable and challenging control over the structure and morphology of their condensed phase. Rather than resorting to chemical modifications or advanced thin-film manufacturing methods such as chemical vapor deposition, the so-called metal-organic framework (MOF) approach is employed to create a highly photoresponsive, nanographene-based thin film employing a layer-by-layer, liquid-phase epitaxy method. It is demonstrated that the novel Cu-HBC MOF thin film exhibits excellent photoresponsive behavior under ultraviolet illumination, including a fast response time ($^<$ 0.02 s) and high current switching ratio ($\approx 10^4$), which significantly outperforms an isostructural MOF Zn-HBC. Furthermore, it is demonstrated that the metal nodes inside the MOF can be used to enhance the photoresponse by efficient exciton splitting.

Z. Xu, Y. Liu, A. Chandresh, L. Heinke, C. Wöll
Institute of Functional Interfaces (IFG)
Karlsruhe Institute of Technology (KIT)
Hermann-von-Helmholtz-Platz 1
76344 Eggenstein-Leopoldshafen, Germany
E-mail: christof.woell@kit.edu
P. B. Pati, V. Monnier, F. Odobel, S. Diring
Universite Lunam
Universite de Nantes
CNRS
Chimie et Interdisciplinarite Synthese Analyse Modelization (CEISAM)
UMR 6230, 2 rue de la Houssiniere, Nantes cedex 3 44322, France
E-mail: Stephane.Diring@univ-nantes.fr
R. Haldar
Tata Institute of Fundamental Research Hyderabad
Gopanpally, Hyderabad, Telangana 500046, India
E-mail: riteshhaldar@tifrh.res.in

1. Introduction

Organic chromophores, in particular polycyclic aromatic molecules, are of high significance towards applications in optoelectronics.[1] The extended, delocalized π-electron structure of these chromophores results in small optical band gaps and high light absorption efficacy. A handful of these organic compounds, such as anthracene, pentacene, perylene, and coronene, have been extensively investigated for their potential in light-emitting diodes, transistors, and solar cell technologies.[2] For these applications, various device manufacturing techniques have been honed over time. Simultaneously, innovative chemical alteration strategies have been devised to adapt the chromophores for the integration into device construction. Even though chemical functionalization is useful, it can inadvertently affect the molecular packing in the associated molecular solids, potentially leading to undesired and unpredictable changes in optical and electronic properties.[3] Moreover, the condensed phase of these chromophores can often adopt more than one structure with similar energies, a phenomenon known as polymorphism, which makes correlating structures and properties a complex task. In addition, in the case of polymorphism grain boundaries between the different phases can have a negative effect on transport properties. Unfortunately, these problems are more the norm than the anomaly in self-assembled materials.[4] For planar aromatic chromophores, π-π interactions generally favor aggregate formation, where planar stacking leads to a quenching of optical excitations.[5]
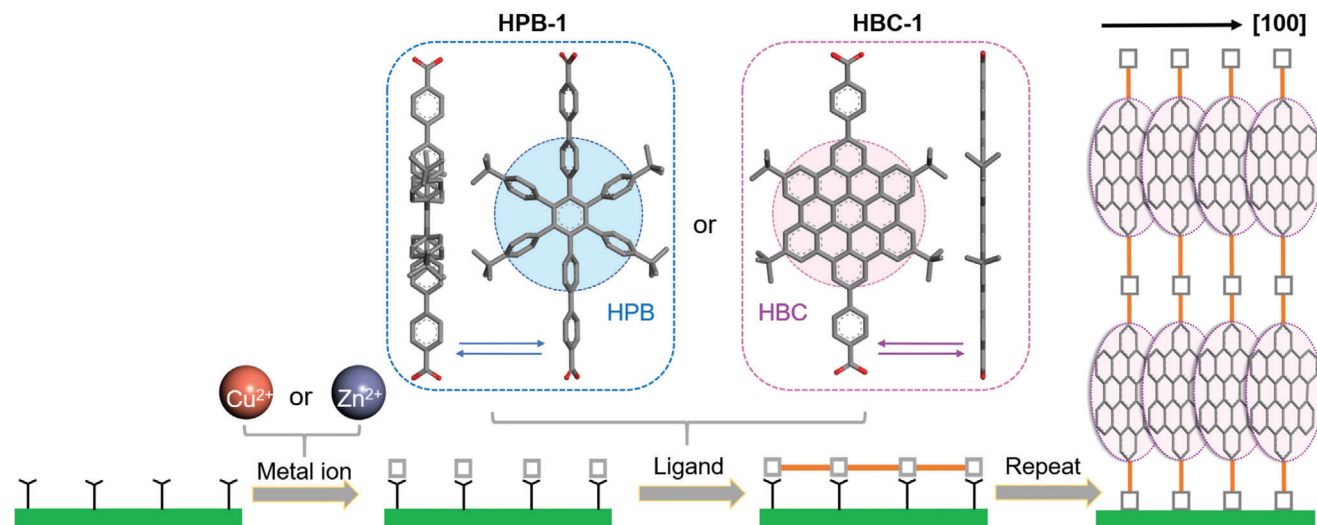
To establish a more predictable relationship between structure and properties, employing the metal-organic framework (MOF) approach has been proven as an efficient instrument.[6] MOFs are assembled from di- or polytopic organic linkers and metal nodes, which can be ions or oxo-clusters.[7] The specific geometry of these linkers and metal nodes dictates the packing of linkers and the spatial distance. Due to the crystalline nature of MOFs, anticipating and adjusting the optical and electronic properties related to the linker using computational methods is comparatively straightforward and can be done using simulation workflows.[8] In principle, any polycyclic

**ADVANCED
SCIENCE NEWS**

www.advancedsciencenews.com

**ADVANCED
FUNCTIONAL
MATERIALS**

www.afm-journal.de

Scheme 1. Schematic illustration of the layer-by-layer synthesis of HPB-1 and HBC-1 linker-based SURMOFs.

aromatic compound can be turned into MOF linker using an appropriate functionalization strategy,[9] thereby enabling the tuning of their properties by creating a specific MOF topology.[10] This MOF approach has been very effective; using MOFs' very high electronic conductivity,[11] efficient and anisotropic energy transfer,[12] charge transfer,[13] light-emitting diodes and transistors have been reported.[14] Although the most prevalent form of MOFs, polycrystalline powders, somewhat restricts their potential for optical applications, various methods have been developed to achieve optical quality in the production of MOF thin films.[6e]

In this work, we have explored a well-known polycyclic aromatic molecule, hexa-*peri*-hexabenzocoronene (HBC), also known as nanographene.[15] Nanographene, has a tendency to aggregate due to strong π-π stacking interactions. This π-π stacking often leads to the formation of tightly packed layers or stacks, much like the arrangement seen for its larger counterpart graphene. This leads to strong electronic coupling with unwanted effects, e.g., the quenching of optical excitations.[16] In this context, the orientations of the molecular transition dipole moments for the corresponding electronic transitions serve as the determining factor. MOFs containing HBC as linker have been described in recent publication.[17] However, the powder form presents challenges when it comes to incorporating them into a device setup. To tackle this issue, we have used a method known as layer-by-layer (lbl) deposition.[18] This technique has been previously leveraged to create highly-defined MOF thin films for different kinds of organic semiconductors.[19] The key first step for the MOF approach is the —COOH functionalization of HBC to yield a ditopic linker (HBC-1). We have used Cu^{2+} and Zn^{2+}-based nodes to assemble oriented MOF thin films with high structural quality. We utilized the same method for nonannulated HBC, hexaphenylbenzene (HPB). In the subsequent sections, we delve into the process and photophysical attributes of these innovative surface-anchored MOF thin films, or SURMOFs. Comparison of the Cu and Zn-HBC thin films reveals that under ultraviolet-illumination Cu-HBC exhibits very high current response, making it suitable for efficient photodetector
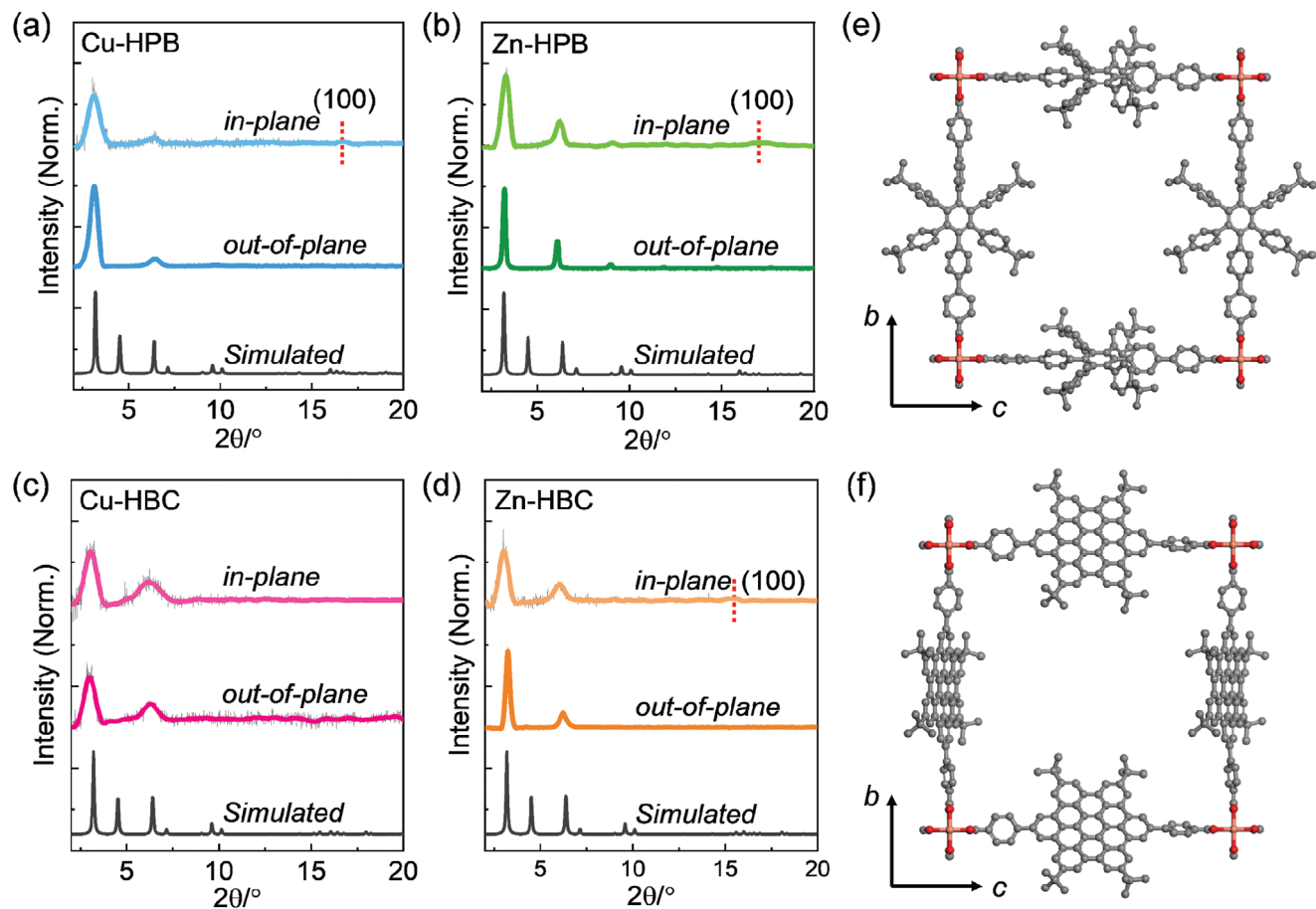
applications. These characteristics of the SURMOFs are discussed in the following.

2. Results and Discussion

The synthesis of the HBC-1 and nonannulated HPB-1 ditopic linkers was described in the supporting information (Figure S1–S9, Supporting Information). HBC-1 has a planar structure, while HPB-1 is a propeller-shaped molecule. The peripheral phenyl rings in HPB-1 can rotate freely, even though the rotational degrees of freedom are limited by the steric hindrance.[20]

A lbl method was used to grow SURMOFs of HPB-1 and HBC-1 using either Cu^{2+} or Zn^{2+}-based nodes (**Scheme 1**). Out-of-plane and in-plane X-ray diffraction (XRD) patterns shown in **Figure 1**a–d reveal that all the four SURMOFs (Cu-HPB, Zn-HPB, Cu-HBC, Zn-HBC) are isostructural. We first focus on Cu-HPB, for which out-of-plane XRD diffraction peaks are found at ~3.2, 6.4, and 9.6°. The in-plane XRD pattern also shows same diffraction peaks, with an additional peak at 16.6°. We used a structural model assuming a SURMOF-2 structure (Figure 1e), in analogy to previously reported systems,[21] where square-grid shaped 2D layers formed by connecting Cu^{2+} dimers (paddle-wheels) via the ditopic linkers. These 2D layers are stacked parallel to the plane of the substrate, as shown in Scheme 1. We used the SIMstack software package to refine this structural model.[22] The structural refinement yielded square grid lattice dimensions of 2.76 nm × 2.76 nm. The inter-layer distance was adjusted to 0.53 nm to reproduce the in-plane XRD-peak at 16.6°. The XRD pattern simulated for this structural model is in agreement with the experimental data.

A similar SURMOF-2 structure was predicted for HBC-SURMOFs (Figure 1f). A closer inspection of the structure reveals a stacking of the HBC cores with a distance of 0.58 nm (Figure S10, Supporting Information), which is slightly larger than that found in the crystalline form of HBC (0.51 nm).[15f] The presence of paddle-wheel nodes in these structures is confirmed by infrared reflection absorption spectroscopy (IRRAS) (Figure S11, Supporting Information). The —COO symmetric

**ADVANCED
SCIENCE NEWS**

www.advancedsciencenews.com

**ADVANCED
FUNCTIONAL
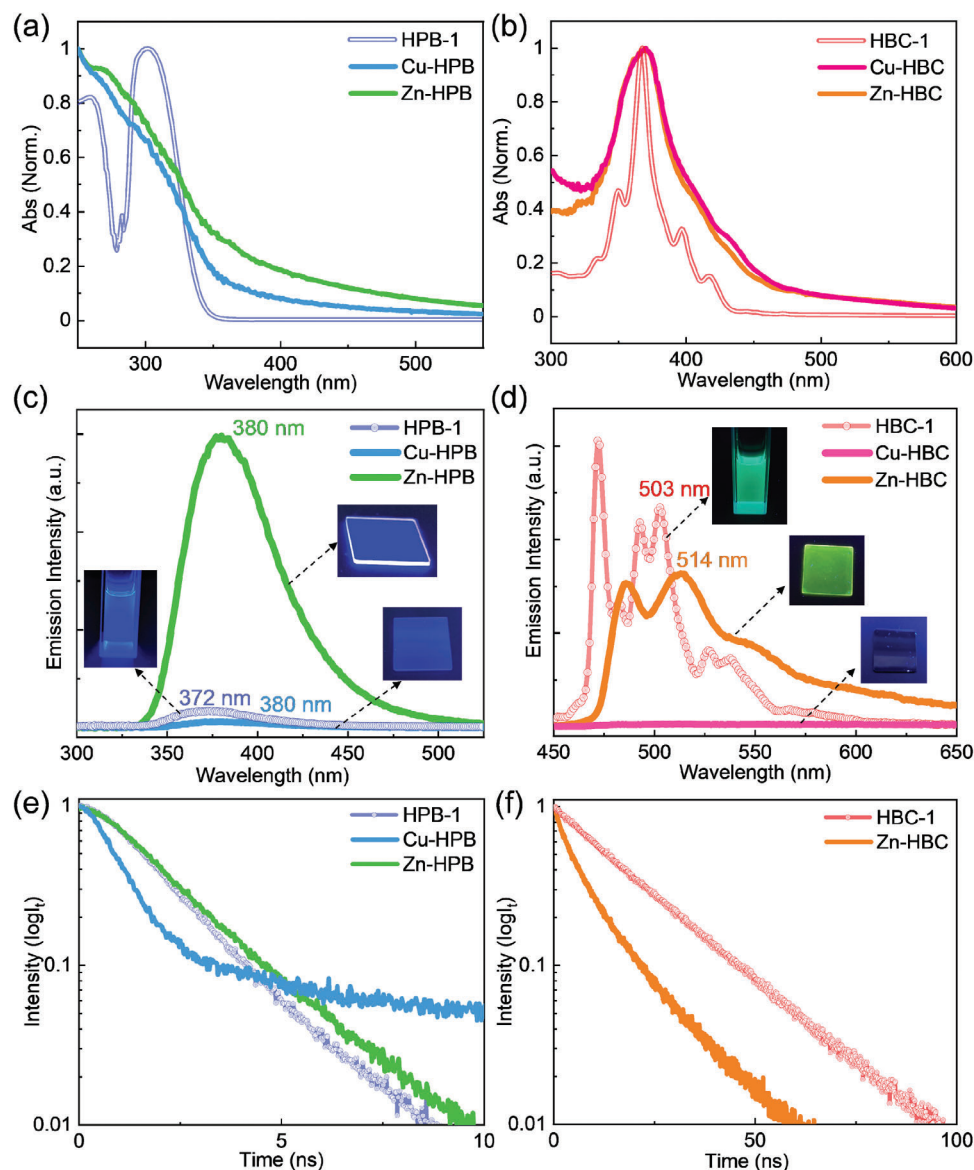MATERIALS**

www.afm-journal.de

Figure 1. Out-of-plane and in-plane XRD patterns of a) Cu-HPB, b) Zn-HPB, c) Cu-HBC and d) Zn-HBC. Structures of e) Cu-HPB and f) Cu-HBC (Cu pink, O red, C grey).

and asymmetric stretching vibrations were observed at 1607 and 1415 cm^{-1}, respectively. These frequencies are characteristic for the paddle-wheel nodes.[23] Scanning electron microscopy (SEM) images confirm that all the thin films exhibited a homogeneous and continuous morphology (Figure S12, Supporting Information).

In these proposed SURMOF-2 type structures of HPB-1 and HBC-1, the aromatic chromophores form stacks running parallel to the plane of the substrate, and pronounced inter-linker interactions are expected to take place.[12b,24] The influence of this stacking on the photophysical properties was determined by measuring optical absorption and photoluminescence of the solvated linkers and the corresponding SURMOFs (**Figure 2**). For HPB-1 in the solvated state (1×10^{-5} M in ethanol), the absorption peak at ≈302 nm indicates the π-π* transition (Figure 2a). In the Cu and Zn-HPB SURMOFs, the absorption bands were found to be broadened, which is common for MOFs due to the coordination between organic linkers and metal nodes as well as the regular arrangement of the organic linkers.[25] For the HBC-case also similar difference was observed, as shown in Figure 2b. These observations confirm the presence of strong inter-linker interactions within the stacks present in the SURMOF structure.[26] The steady-state and time-resolved photoluminescence spectra of the SURMOFs also support this fact, as illustrated in

Figure 2c–f. Compared to the solvated-state HPB-1 emission, Zn-HPB exhibited red-shifted (≈8 nm) and long-lived emission (≈2.73 ns). While the absorption spectra of the Cu- and Zn-based HPB SURMOFs were rather similar, the emission for the Cu-based thin films was drastically reduced relative to the Zn case. In the case of HBC-1, Zn-HBC exhibited a clearly red-shifted emission with shorter lifetime (HBC-1: ≈18.31 ns and Zn-HBC: ≈5.58 ns). For Cu-HBC, a pronounced quenching of luminescence was observed, as in the case of Cu-HPB.

The reason of the enhanced emission efficiency in Zn-HPB compared to the solvated HPB-1 is the inter-HPB-1 interactions within the crystalline framework, which substantially constrain the rotational degrees of freedom of the phenyl groups and thus reduce nonradiative decay.[14b,20,27] For Zn-HBC, the shifted and slightly suppressed emission in comparison to the solvated HBC-1 also confirms the linker-linker electronic interactions in the SURMOF-2 type structure. The strong suppression of the luminescence in the case of the Cu-nodes compared to the Zn-nodes, for both, HBC and HPB, cannot be due to differences in stacking of the chromophores since the corresponding XRD-data reveal that the structural parameters of the two MOF structures are almost identical. We relate this important observation to ligand-to-metal charge transfer (LMCT) for the Cu case. While for Zn^{2+} dimers LMCT is not possible because of the fully filled

**ADVANCED
SCIENCE NEWS**

www.advancedsciencenews.com

**ADVANCED
FUNCTIONAL
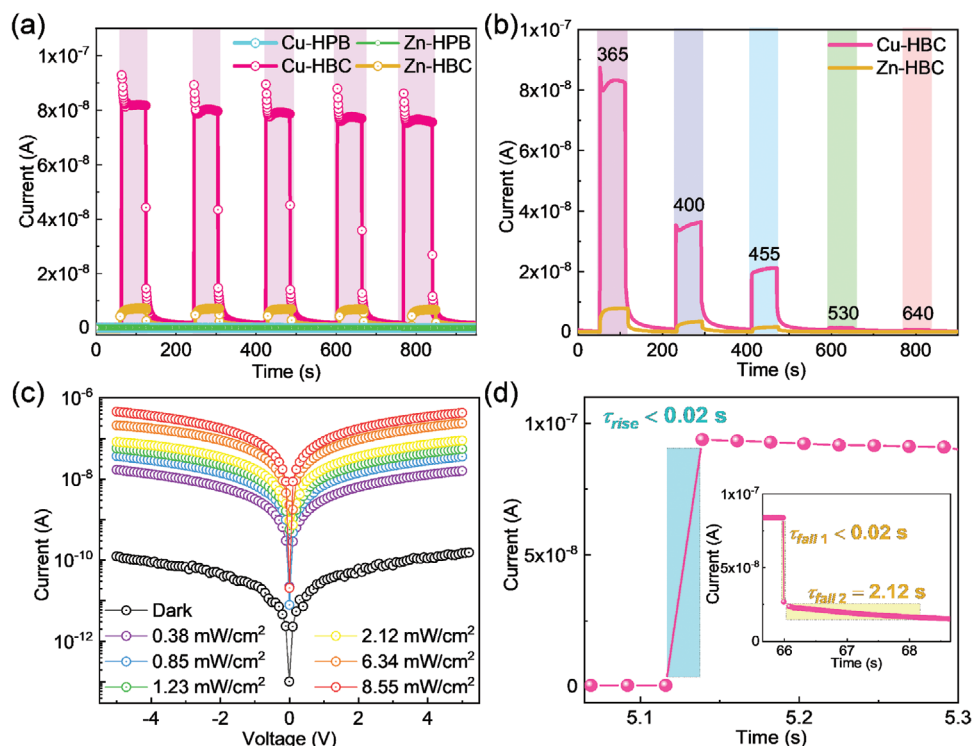MATERIALS**

www.afm-journal.de

Figure 2. Photophysical properties of linkers in the solvated state and after assembly into SURMOFs. a,b) Optical absorption spectra. c,d) Emission spectra, inset: photographs of SURMOFs on quartz substrates under ultraviolet light. e,f) Time-resolved photoluminescence decay profiles.

Zn d-orbitals, for the Cu^{2+} dimers a number of low-lying d-d transitions exist.[28] Note that dipole transitions within the Cu^{2+} dimers are dipole-forbidden,[29] thus strongly reducing radiative transitions and thus remission of visible light.

In the next step, we fabricated devices by growing SURMOFs on Au-patterned glass substrates (see supporting information). We have investigated the photoresponse of the thin films by measuring the current under photoirradiation. Because of the strong π-π interaction among the linkers, we anticipated that photogenerated charge carriers (holes) can delocalize along the stacking direction,[24] leading to efficient photoconduction behavior. To test this, device current was measured at 365 nm light illumination (**Figure 3**a). Among the four SURMOFs, only HBC-SURMOFs exhibited distinct photoresponse. Compared to the Zn-HBC, Cu-HBC exhibited superior response, as photoexcita-

tion enhanced the current by 3 orders of magnitudes (Figure S13 and S14, Supporting Information). This result confirms that free charge carriers (holes) are more mobile in Cu-HBC. The fact that the conductivity enhancement is due to the light-absorption is confirmed by recording the current response under different wavelengths of light irradiation, as shown in Figure 3b. Maximum current enhancement was observed for 365 nm light, according to the maximum light absorption efficiency.[30] The current-voltage (I–V) characteristics for HBC-SURMOFs were measured using 365 nm light source with different power densities. As shown in Figure 3c, the obtained dark current of Cu-HBC thin film was estimated to be 1.10×10^{-10} A. Upon light illumination, photocurrent rises with the increasing illumination power, and it climbs to 4.58×10^{-7} A at 8.55 mW cm^{-2}. The extremely low dark current and the high photocurrent contribute

**ADVANCED
SCIENCE NEWS**

www.advancedsciencenews.com

**ADVANCED
FUNCTIONAL
MATERIALS**

www.afm-journal.de

Figure 3. a) Time-dependent photocurrent response of all SURMOFs under chopped light irradiation of 365 nm with 2.12 mW cm^{-2} at a bias voltage of 5 V. All the samples were deposited for 80 cycles. b) Time-dependent photocurrent of HBC-based SURMOFs under chopped light irradiation of different wavelengths with identical light power. c) Current-voltage curves for Cu-HBC SURMOF under 365 nm with different incident light intensities. d) Rise time and fall time (insert) curves for Cu-HBC SURMOF.

to a considerable switching ratio of $\approx 4.2 \times 10^3$, significantly outperforming Zn-HBC (switching ratio:43, Figure S15, Supporting Information) and exceeding the values reported for the majority of MOF thin films (Table S1, Supporting Information).[31]

The photoresponse time for Cu-HBC thin film was found to be faster, ≈ 20 ms, compared to most of the MOF thin films (Figure 3d; Table S1, Supporting Information).[32] Such efficient and fast photoresponse behavior from the Cu-HBC thin film is unprecedented, and can be attributed to the following factors: i) favorable π-π stacking of the HBC linkers allows fast and efficient delocalization of photogenerated charges, not feasible for the HPB linkers, ii) a photo-induced LMCT process between electron-rich HBC and the Cu^{2+} dimers, which is not possible in the case of Zn^{2+} (see discussion above). We speculate that the strong LMCT for the Cu^{2+} case is not only responsible for the luminescence quenching in the case of the Cu-HBC SURMOFs (see above), but also leads to a more efficient charge separation, with the excited electron tunneling from the HBC linkers into empty d-orbitals of the Cu^{2+} dimer and the hole remaining in the chromophore.

3. Conclusion

In conclusion, a novel HBC chromophore-based MOF thin film exhibiting efficient and fast photocurrent response has been synthesized using a layer-by-layer synthesis method. A major challenge in assembling such large polycyclic aromatic chromophore in thin film geometry is the strong aggregation among the chromophores. Using the MOF approach, in combination with a layer-by-layer deposition method, we were able to fabricate optical quality, homogeneous and oriented thin films. Using appropriately modified chromophores, HBC and also the related nonannulated aromatic chromophore (HPB) were assembled into a crystalline framework. The strong electronic interactions between chromophores in the SURMOFs become evident when the SURMOF absorption and emission spectra are compared to those of the solvated MOF linkers. While good values for the photoconductivity are observed for the Zn-based SURMOFs, interestingly for the Cu-nodes, despite a strongly decreased luminescence, the photoconduction performance (switching ratio as well as response time) is increased to values where the Cu-HBC-SURMOF outperforms other MOFs. We explain the beneficial effect of the Cu-nodes by a strongly enhanced exciton splitting, resulting from an efficient ligand-to-metal charge transfer. The details of this mechanism enhancing electron-hole separation will be investigated in future work.

4. Experimental Section

Synthesis of Cu/Zn-HPB and Cu/Zn-HBC: All the SURMOFs were fabricated by a spin-coating method in a layer-by-layer fashion on functionalized substrates. Quartz substrates were treated with plasma under oxygen for 15 minutes to remove the organic impurities and generate a surface with —OH functional groups. The gold substrate (100-nm Au/2-nm Ti evaporated on Si wafers) was functionalized with 16-mercaptohexadecanoic acid terminated SAM, then rinsed with absolute

ADVANCED
SCIENCE NEWS

www.advancedsciencenews.com

ADVANCED
FUNCTIONAL
MATERIALS

www.afm-journal.de

ethanol and dried under nitrogen. Quartz substrates were used for optical measurements, including absorption and emission measurements. Au substrates were used for IRRAS measurements. Interdigitated gold electrodes were utilized for photoconduction measurements. For Cu/Zn-HPB SURMOFs, ethanolic solution of copper or zinc acetate (1×10^{-3} M) acts as metal solution and HPB-1 (1×10^{-5} M in ethanol) acts as linker source. For Cu/Zn-HBC SURMOFs, copper or zinc acetate (1×10^{-3} M in ethanol) was chosen as metal ion source, while HBC-1 (1×10^{-5} M in ethanol) was chosen as linker source. Metal and linker solutions were sequentially deposited onto the functionalized substrates, each step followed by a washing step with ethanol (for 10 s) to remove unreacted metal/linker or by-products from the surface. For metal and linker both, the spin-coating time was fixed as 10 s with a rotational speed of 2000 revolutions per minute. The thickness of film was controlled by the number of deposition cycles. For the samples used for XRD, UV-vis, and photoluminescence measurements 50 deposition cycles were used.

Supporting Information

Acknowledgements

Conflict of Interest

The authors declare no conflict of interest.

Data Availability Statement

The data that support the findings of this study are available in the supplementary material of this article.

Keywords

[1] Q. Li, Y. Zhang, Z. Xie, Y. Zhen, W. Hu, H. Dong, *J. Mater. Chem. C* **2022**, *10*, 2411.

[2] a) Y.-H. Chen, V. S. Nguyen, H.-H. Chou, Y. S. Tingare, T.-C. Wei, C.-Y. Yeh, *ACS Appl. Energy Mater.* **2020**, *3*, 5479; b) Z. Liu, T. Yu, Z. Wan, Y. Wang, Z. Li, J. Yin, X. Gao, Y. Xia, Z. Liu, *Adv. Electron. Mater.* **2022**, *8*, 2101342; c) J. Cao, S. Yang, *RSC Adv.* **2022**, *12*, 6966. d) J. E. Anthony, *Angew. Chem., Int. Ed.* **2008**, *47*, 452. e) J. Wu, W. Pisula, K. Müllen, *Chem. Rev.* **2007**, *107*, 718.

[3] a) O. L. Griffith, J. E. Anthony, A. G. Jones, Y. Shu, D. L. Lichtenberger, *J. Am. Chem. Soc.* **2012**, *134*, 14185; b) R. Regar, K. S. Mehra, R. Bhowal, J. Sankar, *Eur. J. Org. Chem.* **2019**, *2019*, 6278.

[4] K. S. Mali, M. G. Schwab, X. Feng, K. Müllen, S. D. Feyter, *Phys. Chem. Chem. Phys.* **2013**, *15*, 12495.

[5] a) J. Mei, N. L. C. Leung, R. T. K. Kwok, J. W. Y. Lam, B. Z. Tang, *Chem. Rev.* **2015**, *115*, 11718; b) R. Haldar, A. Mazel, R. Joseph, M. Adams, I. A. Howard, B. S. Richards, M. Tsotsalas, E. Redel, S. Diring, F. Odobel, C. Wöll, *Chem. Eur. J* **2017**, *23*, 14316; c) Y. Huang, J. Xing, Q. Gong, L.-C. Chen, G. Liu, C. Yao, Z. Wang, H.-L. Zhang, Z. Chen, Q. Zhang, *Nat. Commun.* **2019**, *10*, 169.

[6] a) C.-C. Chueh, C.-I. Chen, Y.-A. Su, H. Konnerth, Y.-J. Gu, C.-W. Kung, K. C. W. Wu, *J. Mater. Chem. A* **2019**, *7*, 17079; b) M. D. Allendorf, R. Dong, X. Feng, S. Kaskel, D. Matoga, V. Stavila, *Chem. Rev.* **2020**, *120*, 8581; c) V. Stavila, A. A. Talin, M. D. Allendorf, *Chem. Soc. Rev.* **2014**, *43*, 5994; d) D. E. Williams, N. B. Shustova, *Chem. Eur. J* **2015**, *21*, 15474; e) R. Haldar, L. Heinke, C. Wöll, *Adv. Mater.* **2019**, *32*, 1905227.

[7] H. Furukawa, K. E. Cordova, M. O'Keeffe, O. M. Yaghi, *Science* **2013**, *341*, 1230444.

[8] a) R. Haldar, A. Mazel, M. Krstic, Q. Zhang, M. Jakoby, I. A. Howard, B. S. Richards, N. Jung, D. Jacquemin, S. Diring, W. Wenzel, F. Odobel, C. Wöll, *Nat. Commun.* **2019**, *10*, 2048; b) E. Zojer, C. Winkler, *J. Phys. Chem. Lett.* **2021**, *12*, 7002; c) M. Mostaghimi, C. R. C. Rêgo, R. Haldar, C. Wöll, W. Wenzel, M. Kozlowska, *Front. Mater.* **2022**, *9*, 840644.

[9] a) G. Xing, J. Liu, Y. Zhou, S. Fu, J. J. Zheng, X. Su, X. Gao, O. Terasaki, M. Bonn, H. I Wang, L. Chen, *J. Am. Chem. Soc.* **2023**, *145*, 8979; b) R. Dong, Z. Zhang, D. C. Tranca, S. Zhou, M. Wang, P. Adler, Z. Liao, F. Liu, Y. Sun, W. Shi, Z. Zhang, E. Zschech, S. C. B. Mannsfeld, C. Felser, X. Feng, *Nat. Commun.* **2018**, *9*, 2637.

[10] a) P. Deria, J. Yu, T. Smith, R. P. Balaraman, *J. Am. Chem. Soc.* **2017**, *139*, 5973; b) P. Deria, J. Yu, R. P. Balaraman, J. Mashni, S. N. White, *Chem. Commun.* **2016**, *52*, 13031.

[11] a) X. Liu, M. Kozlowska, T. Okkali, D. Wagner, T. Higashino, G. Brenner-Weiss, S. M. Marschner, Z. Fu, Q. Zhang, H. Imahori, S. Brase, W. Wenzel, C. Wöll, L. Heinke, *Angew. Chem., Int. Ed.* **2019**, *58*, 9590; b) L. S. Xie, G. Skorupskii, M. Dinca, *Chem. Rev.* **2020**, *120*, 8536; c) C. Li, H. Schopmans, L. Langer, S. Marschner, A. Chandresh, J. Burck, Y. Tsuchiya, A. Chihaya, W. Wenzel, S. Bräse, M. Kozlowska, L. Heinke, *Angew. Chem., Int. Ed.* **2023**, *62*, e202217377.

[12] a) J. Yu, R. Anderson, X. Li, W. Xu, S. Goswami, S. S. Rajasree, K. Maindan, D. A. Gomez-Gualdron, P. Deria, *J. Am. Chem. Soc.* **2020**, *142*, 11192; b) R. Haldar, M. Jakoby, A. Mazel, Q. Zhang, A. Welle, T. Mohamed, P. Krolla, W. Wenzel, S. Diring, F. Odobel, B. S. Richards, I. A. Howard, C. Wöll, *Nat. Commun.* **2018**, *9*, 4332.

[13] a) A. Van Wyk, T. Smith, J. Park, P. Deria, *J. Am. Chem. Soc.* **2018**, *140*, 2756; b) R. Haldar, R. Matsuda, S. Kitagawa, S. J. George, T. K. Maji, *Angew. Chem., Int. Ed.* **2014**, *53*, 11772; c) R. Haldar, A. Ghosh, T. K. Maji, *Chem. Commun.* **2023**, *59*, 1569.

[14] a) M. Gutiérrez, C. Martín, M. Van der Auweraer, J. Hofkens, J. C. Tan, *Adv. Optical Mater.* **2020**, *8*, 2000670; b) R. Haldar, M. Jakoby, M. Kozlowska, M. Rahman Khan, H. Chen, Y. Pramudya, B. S. Richards, L. Heinke, W. Wenzel, F. Odobel, S. Diring, I. A. Howard, U. Lemmer, C. Wöll, *Chem. - Eur. J.* **2020**, *26*, 17016; c) G. Wu, J. Huang, Y. Zang, J. He, G. Xu, *J. Am. Chem. Soc.* **2017**, *139*, 1360; d) Z. G. Gu, S. C. Chen, W. Q. Fu, Q. Zheng, J. Zhang, *ACS Appl. Mater. Interfaces* **2017**, *9*, 7259.

[15] a) Y. Gu, Z. Qiu, K. Müllen, *J. Am. Chem. Soc.* **2022**, *144*, 11499; b) A. Narita, X. Y. Wang, X. Feng, K. Müllen, *Chem. Soc. Rev.* **2015**, *44*, 6616; c) Y. Z. Tan, S. Osella, Y. Liu, B. Yang, D. Beljonne, X. Feng, K. Müllen, *Angew. Chem., Int. Ed.* **2015**, *54*, 2927; d) P. Herwig, C. W. Kayser, K. Müllen, H. W. Spiess, *Adv. Mater.* **1996**, *8*, 510; e) H. Seyler, B. Purushothaman, D. J. Jones, A. B. Holmes, W. W. H. Wong,

Pure Appl. Chem. **2012**, *84*, 1047; f) R. Goddard, M. W. Haenel, W. C. Herndon, C. Krüger, M. Zander, *J. Am. Chem. Soc.* **1995**, *117*, 30.

[16] a) D. Wasserfallen, M. Kastler, W. Pisula, W. A. Hofer, Y. Fogel, Z. Wang, K. Müllen, *J. Am. Chem. Soc.* **2006**, *128*, 1334; b) W. W. H. Wong, J. Subbiah, S. R. Puniredd, B. Purushothaman, W. Pisula, N. Kirby, K. Müllen, D. J. Jones, A. B. Holmes, *J. Mater.Chem.* **2012**, *22*, 21131.

[17] S. Suginome, H. Sato, A. Hori, A. Mishima, Y. Harada, S. Kusaka, R. Matsuda, J. Pirillo, Y. Hijikata, T. Aida, *J. Am. Chem. Soc.* **2019**, *141*, 15649.

[18] O. Shekhah, H. Wang, S. Kowarik, F. Schreiber, M. Paulus, M. Tolan, C. Sternemann, F. Evers, D. Zacher, R. A. Fischer, C. Wöll, *J. Am. Chem. Soc.* **2007**, *129*, 15118.

[19] J. Liu, C. Wöll, *Chem. Soc. Rev.* **2017**, *46*, 5730.

[20] R. Hu, J. W. Lam, Y. Liu, X. Zhang, B. Z. Tang, *Chem. - Eur. J.* **2013**, *19*, 5617.

[21] J. Liu, B. Lukose, O. Shekhah, H. K. Arslan, P. Weidler, H. Gliemann, S. Brase, S. Grosjean, A. Godt, X. Feng, K. Müllen, I. B. Magdau, T. Heine, C. Wöll, *Sci. Rep.* **2012**, *2*, 921.

[22] SimStack. The Boost for Computer Aided-Design of Advanced Materials, https://www.simstack.de/, **2023**.

[23] J. L. Zhuang, M. Kind, C. M. Grytz, F. Farr, M. Diefenbach, S. Tussupbayev, M. C. Holthausen, A. Terfort, *J. Am. Chem. Soc.* **2015**, *137*, 8237.

[24] R. Haldar, M. Kozlowska, M. Ganschow, S. Ghosh, M. Jakoby, H. Chen, F. Ghalami, W. Xie, S. Heidrich, Y. Tsutsui, J. Freudenberg,

S. Seki, I. A. Howard, B. S. Richards, U. H. F. Bunz, M. Elstner, W. Wenzel, C. Wöll, *Chem. Sci.* **2021**, *12*, 4477.

[25] Y. Cui, Y. Yue, G. Qian, B. Chen, *Chem. Rev.* **2012**, *112*, 1126.

[26] J. S. Qin, S. Yuan, L. Zhang, B. Li, D. Y. Du, N. Huang, W. Guan, H. F. Drake, J. Pang, Y. Q. Lan, A. Alsalme, H. C. Zhou, *J. Am. Chem. Soc.* **2019**, *141*, 2054.

[27] R. Haldar, S. Diring, P. K. Samanta, M. Muth, W. Clancy, A. Mazel, S. Schlabach, F. Kirschhofer, G. Brenner-Weiss, S. K. Pati, F. Odobel, C. Wöll, *Angew. Chem., Int. Ed.* **2018**, *57*, 13662.

[28] M. D. Allendorf, C. A. Bauer, R. K. Bhakta, R. J. Houk, *Chem. Soc. Rev.* **2009**, *38*, 1330.

[29] K. Müller, K. Fink, L. Schöttner, M. Koenig, L. Heinke, C. Wöll, *ACS Appl. Mater. Interfaces* **2017**, *9*, 37463.

[30] Y. B. Tian, N. Vankova, P. Weidler, A. Kuc, T. Heine, C. Wöll, Z. G. Gu, J. Zhang, *Adv. Sci.* **2021**, *8*, 2100548.

[31] a) L.-A. Cao, M.-S. Yao, H.-J. Jiang, S. Kitagawa, X.-L. Ye, W.-H. Li, G. Xu, *J. Mater. Chem. A* **2020**, *8*, 9085; b) H. Arora, R. Dong, T. Venanzi, J. Zscharschuch, H. Schneider, M. Helm, X. Feng, E. Canovas, A. Erbe, *Adv. Mater.* **2020**, *32*, 1907063; c) M. H. Tran, J. Hur, *Adv. Optical Mater.* **2022**, *10*, 2101404.

[32] a) C. K. Liu, V. Piradi, J. Song, Z. Wang, L. W. Wong, E. H. Tan, J. Zhao, X. Zhu, F. Yan, *Adv. Mater.* **2022**, *34*, 2204140; b) X. Shang, I. Song, G. Y. Jung, W. Choi, H. Ohtsu, J. H. Lee, J. Ahn, J. Y. Koo, M. Kawano, S. K. Kwak, J. H. Oh, *J. Mater. Chem. C* **2021**, *9*, 7310.